LIMNOLOGY
and
OCEANOGRAPHY

ASLO

Limnol. Oceanogr. 62, 2017, S348–S363

doi: 10.1002/lno.10654

Submarine groundwater discharge drives biogeochemistry in two Hawaiian reefs

Christina M. Richardson ,[1]* **Henrietta Dulai,**[1] **Brian N. Popp,**[1] **Kathleen Ruttenberg,**[2] **Joseph K. Fackrell**[1]

[1]Department of Geology and Geophysics, School of Ocean and Earth Science and Technology, University of Hawai'i at Mānoa, Honolulu, Hawai'i

[2]Department of Oceanography, School of Ocean and Earth Science and Technology, University of Hawai'i at Mānoa, Honolulu, Hawai'i

Abstract

Groundwater inputs are typically overlooked as drivers of environmental change in coastal reef studies. To assess the impact of groundwater discharge on reef biogeochemistry, we examined two fringing reef environments, located in Maunalua Bay on the south shore of O'ahu, Hawai'i, that receive large inputs of submarine groundwater discharge. We supplemented 25- and 30-d time series measurements of salinity, water temperature, pH, dissolved oxygen, and ^{222}Rn with high-resolution 24-h nutrient, dissolved inorganic carbon (DIC), total alkalinity (TA), and δ^{13}C–DIC measurements to evaluate both groundwater-induced and biologically-driven changes in coastal carbonate chemistry across salinity gradients. Submarine groundwater discharge at these two locations was characterized by low pH_T (7.36–7.62), and variable DIC (1734–3046 μM) and TA (1716–2958 μM) content relative to ambient seawater. Groundwater-driven variability in coastal carbonate system parameters was generally on the same order of magnitude as biologically-driven variability in carbonate system parameters at our study locations. Further, our data revealed a shift in reef metabolism from net dissolution to net calcification across this groundwater-driven physicochemical gradient. At sites with high levels of groundwater exposure, net community production and calcification rates were reduced. Our findings shed light on the importance of considering groundwater inputs when examining coastal carbonate chemistry.

Submarine groundwater discharge (SGD) has been widely documented in coral reefs in Asia (Cardenas et al. 2010; Blanco et al. 2011; Wang et al. 2014), Australia (Stieglitz 2005; Santos et al. 2011), the Caribbean (Lewis 1987; Lapointe et al. 2010), North and Central America (Crook et al. 2012, 2013), and the Pacific (Paytan et al. 2006; Street et al. 2008; Cyronak et al. 2013). SGD consists of both fresh and saline components and is thought to be of the same order of magnitude as riverine discharge worldwide (Moore 2010; Kwon et al. 2014), with the fresh component of SGD estimated to equal 6% of riverine discharge globally (Zektser and Loaiciga 1993). SGD is geochemically distinct and typically enriched in dissolved solutes relative to both fresh surface water and receiving marine waters (Slomp and Van Cappellen 2004), and as a result may affect biochemical functions of coral reef ecosystems where it occurs. The effects of SGD and associated material fluxes on C cycling have been largely overlooked in coastal reef studies, however.

C cycling in reefs can be parameterized using community scale estimates of inorganic (calcification-dissolution) and organic (photosynthesis-respiration) C metabolism. These estimates typically rely on discrete measurements of DIC and TA made over the course of at least a day, with changes in DIC and TA attributed to changes in net community calcification (NCC) and net community production (NCP). To correct for salinity differences, these data are often initially normalized to a reference salinity using the traditional normalization approach (Friis et al. 2003), which does not take into consideration additional inputs of DIC or TA coeval with salinity changes. While traditional normalization of carbonate system parameters can account for physical

*Correspondence: cmrich@hawaii.edu

Additional Supporting Information may be found in the online version of this article.

Special Issue: Headwaters to Oceans: Ecological and Biogeochemical Contrasts Across the Aquatic Continuum
Edited by: Marguerite Xenopoulos, John A. Downing, M. Dileep Kumar, Susanne Menden-Deuer, and Maren Voss

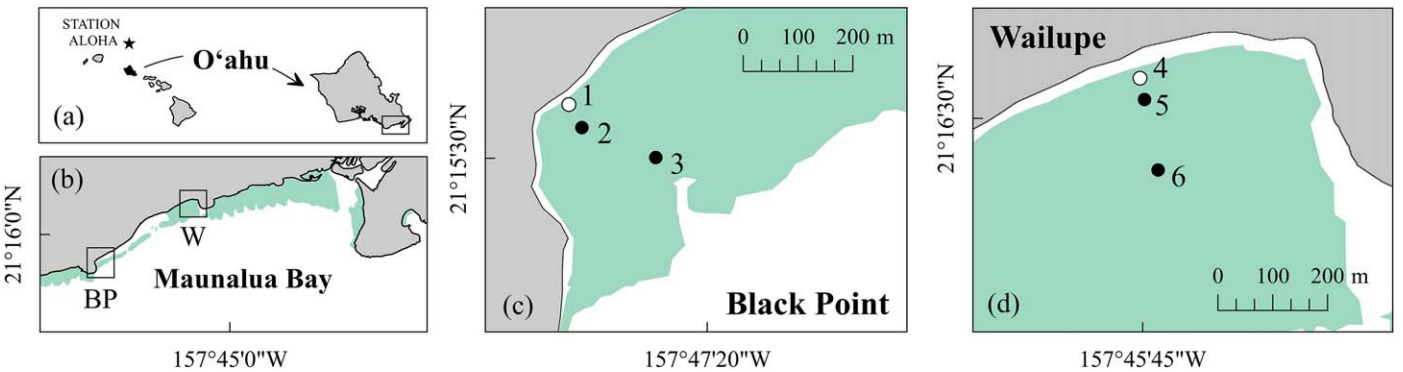

Fig. 1. (**a**) Overview of the Hawaiian Islands and Station ALOHA, and a close-up of the island of O'ahu, with Maunalua Bay framed by a transparent black box, (**b**) Overview of Maunalua Bay and study area locations, Black Point (BP) and Wailupe (W), (**c**) Black Point study location, and (**d**) Wailupe study location. Numbers, 1 to 6, denote sampling sites. The autonomous sampling platform was co-located with site 2 at Black Point and site 4 at Wailupe. Sites closest to the groundwater sources at both locations are indicated by white circular markers. Approximate reef cover is represented by the turquoise regions (modified from University of Hawai'i at Mānoa, Department of Urban and Regional Planning [UH] 2002 and NOAA 2003).

processes such as rainfall and evaporation, this method may not adequately characterize C dynamics in reefs with SGD. SGD contributions to nearshore C reservoirs can be considerable, though few studies exist documenting the carbonate chemistry of SGD. Cyronak et al. (2014) observed SGD into reef environments with TA and DIC concentrations over 2000 μM, and studies from Hawai'i show DIC and TA content in coastal groundwater is commonly over 2000 μM as well (Schopka and Derry 2012; Lantz et al. 2014; Fackrell 2016).

SGD may also indirectly influence reef metabolism. The delivery of inorganic nutrients via SGD can stimulate the production and subsequent remineralization of organic matter in coastal systems (Sunda and Cai 2012), and elevated inorganic nutrient inputs have been shown to reduce calcification in natural settings (e.g., Fabricius 2005) as well as incubation experiments (Marubini 1996; Ferrier-Pagès et al. 2000). SGD in tropical climates often consists of freshwater with low pH and temperature relative to ambient seawater; these physicochemical parameters may act in concert with one another to reduce calcification in reef environments with SGD (Coles and Jokiel 1992; Jokiel et al. 1993; Lough and Barnes 2000; Shaish et al. 2010). The direct (e.g., material fluxes of inorganic C) and indirect (e.g., nutrient inputs and physicochemical gradients) effects of SGD on coastal carbonate chemistry in nearshore ecosystems, such as coral reefs, may be important considerations for future assessments of reef C cycling in areas with SGD.

The present study evaluates how SGD modifies coastal carbonate chemistry in two contrasting Hawaiian coral reef ecosystems, Black Point and Wailupe, on the southeastern coast of O'ahu. Previous studies in this region observed significant differences in both dissolved inorganic N concentrations and N sources in SGD between the two locations (Richardson et al. in press). Effluent from proximal on-site sewage disposal systems mixes with terrestrial groundwater and substantially elevates N loads in SGD at Black Point relative to Wailupe. Differences between these two locations provide a unique opportunity to examine how changes in groundwater geochemistry impact nearshore carbonate chemistry.

We monitored SGD and select geochemical parameters using an autonomous sampling platform over a period of 25- to 30-d to supplement high-resolution 24-h time series measurements of inorganic nutrients and carbonate system parameters at both locations. Using these data, we investigated the effects of spatially-distinct groundwater solute fluxes on coastal carbonate chemistry and reef metabolism. Combined, our findings reveal the interplay between physical and biological controls on nearshore carbonate chemistry and their potential role in regulating NCC and NCP.

Study region

Site details

Maunalua Bay is an 8 km embayment located on the southern shore of the island of O'ahu, Hawai'i, with three primary regions of SGD: Black Point, Kawaikui, and Wailupe (Richardson et al. in press). Two of these groundwater-influenced coastal locations, Black Point and Wailupe, were considered for this study in August (Black Point) and September (Wailupe) of 2015 (Fig. 1). Three sites along roughly shore-perpendicular transects that spanned wide salinity gradients were monitored at each coastal location (Black Point and Wailupe). Site 1 at Black Point was approximately 5 m offshore of the dominant groundwater discharge point, while site 4 at Wailupe was situated within 2 m of the dominant groundwater discharge point. These discharge points are roughly 0.5 m in diameter and appear to be fed by preferential flow of fresh groundwater through fractures and/or other conduits in the underlying bedrock. Both sites also

experience diffuse groundwater seepage from portions of the shoreline. The groundwater springs monitored herein were selected over the seepage faces as they discharge a greater volume of groundwater (Dimova et al. 2012; Swarzenski et al. 2013; Ganguli et al. 2014; Richardson et al. in press). Additionally, since the diffuse seepage and groundwater springs at each study area have similar geochemical endmember compositions (Swarzenski et al. 2013; Richardson et al. in press), groundwater inputs from the springs and seepage faces produce similar mixing profiles with ambient ocean water. However, the groundwater endmembers are not uniform between the two sampling locations. SGD at Black Point and Wailupe originate from separate aquifers, and previous studies have found marked differences in their respective nutrient and trace metal compositions (Swarzenski et al. 2013; Ganguli et al. 2014; Nelson et al. 2015; Richardson et al. in press).

Benthic structure

In general, community structure at both study locations resembles that of an algal dominated reef. Sand, rubble, and macroalgae dominate benthic cover at sites 1 and 2 at Black Point, while coral cover is highest along the outer perimeter of the reef flat (site 3). Blooms of the green macroalgae, *Bryopsis pennata*, persisted in the water column and benthos at all sites during the Black Point sampling event. Benthic cover at Wailupe is dominated by macroalgae, with cover ranging from 30% to 50% on average (Amato 2015). At Wailupe, sand and rubble constitute nearly 20 to 50% of the benthos at all sites, and corals are found predominantly offshore, with cover estimated as 2 to 5% at site 6 (Amato 2015).

Methods

Long-term instrument deployments

A portable NaI(Tl) scintillation detector, or "SGD Sniffer" (Ortec), was used to measure ^{222}Rn in water over 1-h integrated time periods using the method of Dulai et al. (2015). The SGD Sniffer was encased in an aluminum frame and deployed in a stationary position for a period of 30 d at Black Point (10 August 2015–09 September 2015) and 25 d at Wailupe (09 September 2015–04 October 2015). A multiparameter water quality meter (YSI V2-2) was attached to the frame and used to simultaneously monitor salinity (± 0.01 ppt), water temperature (± 0.15°C), dissolved oxygen (DO) (± 0.2 mg L^{-1}), and pH_{NBS} (± 0.2 units) at 15-min intervals. Floats kept the frame buoyant and the sensors at the same depth (0.2 m below sea level) throughout the deployment. A conductivity temperature depth (CTD) diver was affixed to the SGD Sniffer anchor point and used to monitor water depth (± 0.5 cm) at 15-min intervals. Rainfall data was acquired for each sampling period from USAF Station 911820 based out of the Honolulu International Airport, approximately 15 km west of the study locations (http://www.ncdc.noaa.gov/). Corrections and conversions applied to the long-term pH data, which are solely used to provide qualitative reference to the 24-h high-resolution samples, can be found in Supporting Information.

24-h sampling events

Two 24-h sampling events were completed at three coastal sites and the dominant groundwater spring at Black Point (12 August 2015) and Wailupe (27 September 2015) to monitor nutrient, DIC, and TA concentrations as well as salinity and δ^{13}C–DIC values (Fig. 1). Coastal water and groundwater samples were collected every 3 h at Black Point (n = 9 for each site) and every 3 to 6 h at Wailupe (n = 6 for each site). Discrete samples were collected from an approximate depth of 0.2 m below sea level. Coastal sampling sites at each location were selected to capture the full salinity gradient. Site 2 at Black Point and site 4 at Wailupe were colocated with the autonomous sampling platform. Groundwater was sampled via peristaltic pump from a piezometer installed at the dominant submarine spring site at each location (Fig. 1). Photosynthetically active radiation (PAR) was monitored using an Odyssey Logger for the duration of each 24-h sampling event.

Water sample processing

All water samples were originally collected in HCl-cleaned 1 L bottles and subsampled immediately after collection. Water samples for salinity, nutrients, DIC, and TA were analyzed at the University of Hawai'i's SOEST Laboratory for Analytical Biogeochemistry (S-LAB). Nutrient samples were filtered using 0.2 μm nylon filters into 60 mL HCl-cleaned HDPE bottles and analyzed using a Seal Analytical AA3 HR AutoAnalyzer for $NO_3^- + NO_2^-$, PO_4^{3-}, NH_4^+, and SiO_4^{4-}. Ten blind duplicates were partitioned from a total of 80 nutrient samples (Black Point, n = 40, and Wailupe, n = 40). Sample precision at one standard deviation (SD) was as follows: 0.7 μM $NO_3^- + NO_2^-$, 0.02 μM PO_4^{3-}, 0.1 μM NH_4^+, and 9.6 μM SiO_4^{4-}. Salinity samples were analyzed using a Metrohm 856 Conductivity Module and had a sample precision of 0.01 within one SD.

Samples for DIC and TA were sub-sampled into combusted 500 mL borosilicate bottles with 1% headspace and injected with 0.1% by volume of saturated $HgCl_2$ solution to inhibit biological activity. Borosilicate glass stoppers were greased with Apeizon L and secured with tape to ensure that the samples remained gas-tight. DIC concentration was determined using a Marianda VINDTA 3D at the S-LAB, with analytical accuracy evaluated using certified reference materials from A. Dickson at Scripps Institution of Oceanography at the University of California at San Diego (Dickson et al. 2003). All DIC samples were analyzed in duplicate. TA samples were analyzed in triplicate on a Metrohm 905 Titrando using Gran titrations (Gran 1952) at S-LAB. DIC and TA sample accuracy were within 4 μM of certified reference materials. DIC and TA

sample precision within one SD was 0.8 μM and 3.1 μM, respectively.

Water samples for δ^{13}C–DIC analysis were collected in crimp-top 20 mL vials and poisoned with 0.5% by volume of saturated $HgCl_2$ solution to inhibit biological activity. δ^{13}C-DIC values were determined using the method of Salata et al. (2000) and measured using a Thermo Finnigan MAT 252 coupled with a GasBench II interface at the University of Hawai'i's Stable Isotope Biogeochemistry Lab. Results are reported in units of ‰ relative to Pee Dee Belemnite (PDB) and normalized to NBS-18 and NBS-19 International Atomic Energy Agency reference materials using the accepted values of −5.04‰ Vienna Pee Dee Belemnite (VPDB) and 1.95‰ VPDB, respectively. Sample accuracy was 0.2‰, and sample precision within one SD was 0.1‰.

Calculations

^{222}Rn box models

Groundwater endmember ^{222}Rn activities were monitored at both locations during each 24-h sampling period (Black Point, $n = 9$; Wailupe, $n = 6$). These values were used in conjunction with CTD depth data (± 0.5 cm) and ^{222}Rn values from the SGD Sniffer to calculate groundwater advection rates using a transient mass balance box model as described by Dulai et al. (2015). In short, a coastal radon inventory (Bq m^{-2}) was calculated as activity (Bq m^{-3}), which was measured in hourly time steps, multiplied by observed water depth (m). The difference in inventories in each consecutive time step was assumed to be the radon flux to/from the coastal box over the measurement time interval (Bq m^{-2} h^{-1}). The radon flux was corrected for losses by atmospheric evasion, losses by lateral mixing, radon produced in the water column by the decay of its parent, offshore radon contribution during flood tides, and diffusion from bottom sediments (all in Bq m^{-2} h^{-1}). The corrected flux, which is assumed to represent SGD, was divided by the groundwater endmember activity (Bq m^{-3}) to derive water fluxes (m^3 m^{-2} d^{-1}). These rates were up-scaled to location-wide fluxes (m^3 d^{-1}) using the spatial bounds of the extent of the radon plume defined by Richardson et al. (in press). Groundwater material fluxes were calculated using the location-specific mean daily discharge rate and the mean groundwater endmember concentration for each constituent. Constituents were sampled at the discharge point, and therefore represent true concentrations exiting the subterranean estuary and discharging to the reef.

Salinity normalization of geochemical data

Time series groundwater endmember data collected from the 24-h sampling period were used to normalize all geochemical data aside from δ^{13}C–DIC values to a common reference salinity as follows:

$$C_1 = C_{mix} + \left(C_{mix} - C_{sgd}\right)\left((S_{mix} - 35.2)/\left(S_{sgd} - S_{mix}\right)\right) \quad (1)$$

where C_1 is the salinity normalized concentration at the reference salinity (35.2), C_{mix} is the concentration of the groundwater-marine mixture, C_{sgd} is the average groundwater endmember concentration, S_{mix} is the salinity of the groundwater-marine mixture, and S_{sgd} is the average salinity of the groundwater endmember. The reference salinity, 35.2, was established as a marine endmember based on 2014 Station ALOHA sea surface data adapted from Dore et al. (2009).

δ^{13}C–DIC values were salinity normalized to remove the effect of physical mixing with groundwater using:

$$R_{mix} = \left(\left(f_{marine} C_{marine} R_{marine}\right) + \left(f_{gw} C_{gw} R_{gw}\right)\right)/C_{mix} \quad (2)$$

where R_{mix} is the expected isotopic ratio of a groundwater-marine mixture, C_{mix} is the DIC concentration of the mixture, R_{marine} is the isotopic ratio of the marine endmember, C_{marine} is the DIC concentration of the marine endmember, f_{marine} is the marine water fraction, R_{gw} is the average isotopic ratio of the groundwater endmember, C_{gw} is the DIC concentration of the groundwater endmember, and f_{gw} is the groundwater fraction (Sansone et al. 1999). The marine endmember was chosen as the average $^{13}C/^{12}C$ ratio and DIC concentration of the four most saline samples, with two selected from the nighttime sampling period and two selected from the daytime sampling period. The isotopic ratios, R_{mix}, were then converted to δ^{13}C–DIC values using:

$$\delta^{13}\text{C–DIC} = \left(\left(R_{mix} - R_{std}\right)/R_{std}\right)1000 \quad (3)$$

where R_{std} is the isotopic ratio of the standard, VPDB. The difference between the predicted mixed δ^{13}C–DIC values using Eq. 3 and the observed values were considered to represent the salinity normalized aggregate change in δ^{13}C–DIC values due to reef metabolism of C (e.g., $\Delta n\delta^{13}$C–DIC).

Carbonate system parameter determination

CO2SYS (Pierrot et al. 2006) was used to calculate additional carbonate system parameters from discrete sample DIC and TA concentrations based on carbonic acid constants from Mehrback et al. (1973), as refit by Dickson and Millero (1987). We included corresponding sample SiO_4^{4-} and total P concentrations as input parameters since groundwater from our study area had elevated SiO_4^{4-} and total P content relative to ambient seawater. Output temperatures were determined using Onset TidbiT v2 Temp Loggers (± 0.2°C) or Schlumberger CTD divers (± 0.1°C) deployed at each sampling station. Carbonate system parameters were calculated for both in situ and salinity normalized water samples to isolate the effects of physical mixing between groundwater and marine water from overall carbonate system parameters.

NCC and NCP rates

NCC rates were calculated for each time interval at each sampling site relative to the Station ALOHA marine endmember as follows (e.g., Riebesell et al. 2010):

$$\mathrm{NCC} = -0.5(\Delta\mathrm{nTA})(\rho h/\tau) \quad (4)$$

where ΔnTA is the change in salinity normalized TA (nTA) at the coastal sites relative to the marine endmember (mmol kg^{-1}), ρ is the density of water (kg m^{-3}), h is the water height (m), and τ is the residence time (h). Average water column depths were based on CTD diver data from each site. Water residence times (τ) were determined using ^{223}Ra and ^{224}Ra activities (Moore 2000). Residence times were 11.9 h at Black Point and 17.8 h at Wailupe (Supporting Information). These times are supported by the results of Wolanski et al. (2009), which suggest that water residence times are below that of a day in the central (Wailupe) and western (Black Point) regions of Maunalua Bay. Uncertainties on residence times were approximately ± 6.9 h (± 58%) at Black Point and ± 9.0 h (± 50%) at Wailupe (Supporting Information). These errors were similar in magnitude to other reef studies that have used radioisotope tracers to evaluate residence times (Venti et al. 2012; Muehllehner et al. 2016).

NCP rates were subsequently calculated as follows:

$$\mathrm{NCP} = -h\rho(\Delta\mathrm{nDIC} - 0.5\Delta\mathrm{nTA})/\tau - F \quad (5)$$

where ΔnDIC is the change in salinity normalized DIC (nDIC) at the coastal sites relative to the marine endmember (mmol kg^{-1}), and F is the air-sea CO_2 flux (mmol C m^{-2} h^{-1}).

DIC and TA measurement precision was used to calculate when ΔnTA and ΔnDIC were statistically significant. Using the approach of Muehllehner et al. (2016), ΔnTA and ΔnDIC were significant ($t = 0.05$) to ± 2.9 μM and ± 3.0 μM, respectively. All ΔnTA and ΔnDIC values at Wailupe exceeded these thresholds. At Black Point, 93% of ΔnTA and 96% of ΔnDIC measurements were statistically significant.

Uncertainties in NCC and NCP rates were calculated considering errors for water depth, ΔnTA, ΔnDIC, and air-sea CO_2 flux, when appropriate.

Air-sea CO_2 flux

Air-sea CO_2 flux was calculated using the following equation from Wanninkhof (1992):

$$F = ks(\Delta\mathrm{pCO_2}) \quad (6)$$

where F is the air-sea CO_2 flux, k is the gas transfer velocity, s is the solubility of CO_2, and ΔpCO_2 is the difference between air and water pCO_2. The pCO_2 of air used in this calculation was based on globally averaged marine surface annual mean CO_2 data for 2015 (399.45 ± 0.10) (E. Dlugokencky and P. Tans, NOAA/ESRL, www.esrl.noaa.gov/gmd/ccgg/trends/). The solubility of CO_2 was calculated using the equations of Weiss (1974). Gas transfer velocities were estimated using parameterizations from Frankignoulle et al. (1996) as compiled by Borges et al. (2004) and Raymond and Cole (2001). These parameterizations were selected due to their similarity to our study locations' physiographic dynamics (e.g., reefs and estuaries) and dimensions (e.g., depth).

All gas transfer velocities were corrected for the Schmidt number at in situ conditions and normalized to 600 (Wanninkhof 1992). Wind speed data were taken from NOAA Station OOUH1 at 6-min intervals (http://www.ncdc.noaa.gov/) at a height of 8.7 m and corrected to 10 m using the methods of Johnson (1999). Uncertainties on air-sea CO_2 fluxes were calculated by prescribing wind data an average uncertainty of ± 0.3 m s^{-1}, which was based on the reported accuracy of the wind measurements, and by utilizing the following calculated sample precisions within one standard deviation to propagate analytical uncertainty through all subsequent calculations for pCO_2, fCO_2, and [CO_2], respectively: 12 μatm, 12 μtam, and 0.4 μM.

Results

Long-term time series trends

At Black Point, mean salinity was 32.1 ± 2.0, with a range of 21.2 to 35.6 (Fig. 2). Mean salinity at Wailupe was 29.5 ± 3.2 and ranged from 13.2 to 35.2. Water temperature was cooler on average at Wailupe (26.6 ± 1.7), with greater variability compared to Black Point (28.1 ± 1.1°C). The range in pH_T at Wailupe, 7.93 to 8.17, was smaller in magnitude than at Black Point, where minimum and maximum values were 7.61 and 8.38, respectively. Similar to pH_T, DO showed greater variability at Black Point, ranging from 1.6 mg L^{-1} to 16.4 mg L^{-1} compared to 1.5 mg L^{-} to 11.8 mg L^{-1} at Wailupe. Although groundwater inputs at both study areas were temporally variable, location mean groundwater fluxes were relatively similar. Black Point and Wailupe SGD averaged 11700 ± 5900 m^3 d^{-1} and 9100 ± 2700 m^3 d^{-1}, respectively.

High-resolution 24-h time series data

Long-term time series overlap with 24-h time series

Long-term time series salinity and ^{222}Rn data followed changes in tide during each 24-h sampling event at both sites (Fig. 3). As tide rose at Black Point, salinity increased to a daily maximum of 35.6, and ^{222}Rn activities approached detection limits, suggesting that the flux from groundwater springs was minimal between 12:00 to 15:00 (Fig. 3). Similarly, at Wailupe, salinity peaked at 32.9 during high tide and dropped to 13.2 during low tide. Corresponding ^{222}Rn activities reached a maximum of 100 dpm L^{-1} during low tide and a minimum at detection limits during high tide. DO and pH_T generally covaried at both sites, with the highest DO concentrations occurring in concert with maxima in pH_T. At Wailupe, however, the minimum pH_T occurred at approximately 21:00 and was out of sync with DO. This pH_T

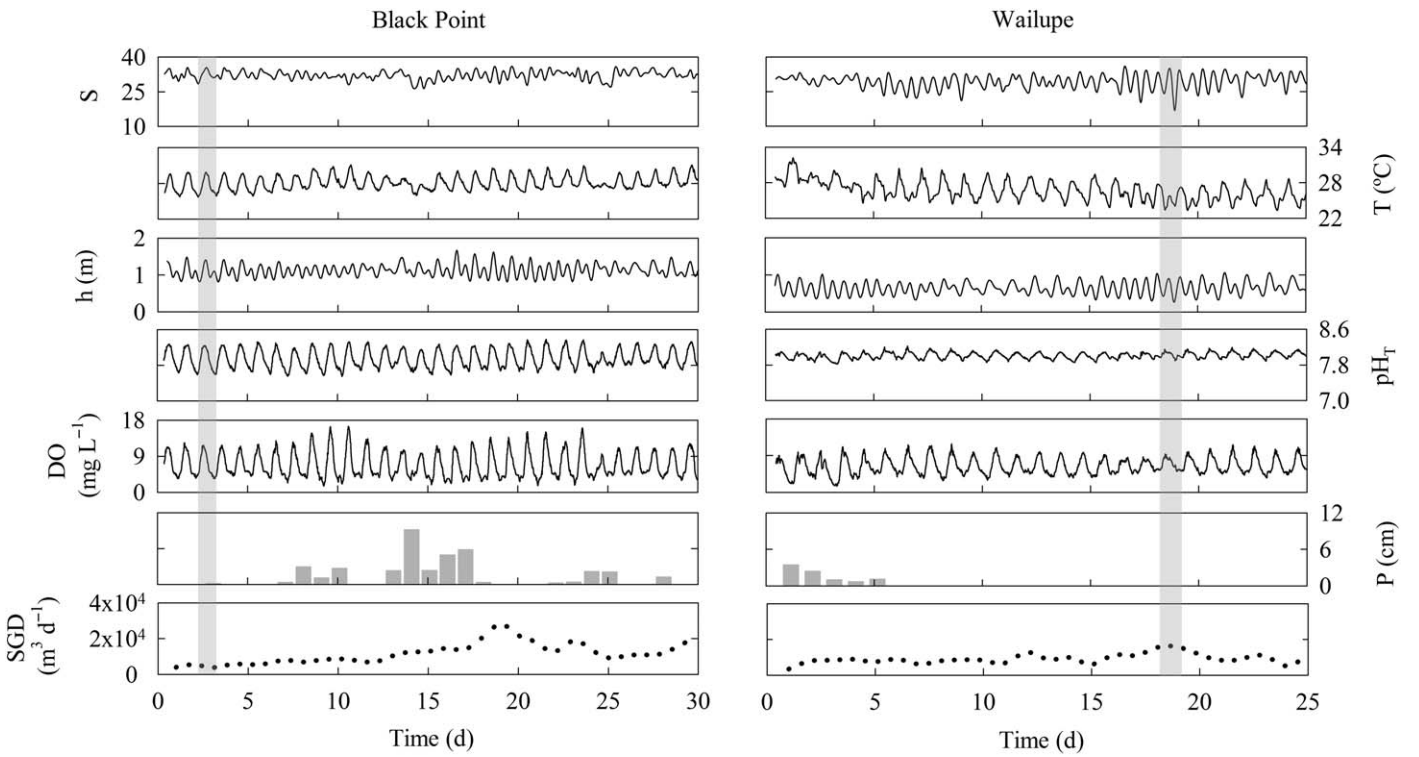

Fig. 2. Time series salinity (S), water temperature (T), water height (h), pH_T, dissolved oxygen (DO), and mean daily SGD for site 2 at Black Point and site 4 at Wailupe. Precipitation (P) data from USAF Station 911820 is included. Shaded areas denote time periods that correspond to the 24-h sampling events. Deployment dates for Black Point and Wailupe were 10 August 2015 to 09 September 2015 and 09 September 2015 to 04 October 2015, respectively.

minimum instead coincided with low tide, when groundwater discharge was greatest, as evidenced by the low salinity and elevated ^{222}Rn activity around 21:00 at Wailupe (Fig. 3). SGD at Black Point and Wailupe averaged 4000 m^3 d^{-1} and 15700 m^3 d^{-1} for each 24-h sampling period, respectively.

Groundwater carbonate chemistry and material fluxes

Groundwater DIC (3038 ± 6 μM) and TA (2946 ± 8 μM) content was elevated at Black Point relative to Station ALOHA and Wailupe (Table 1). As a result, DIC and TA fluxes were greatest at Black Point, with inputs of 36000 mol d^{-1} of DIC and 34000 mol d^{-1} of TA. At Wailupe, groundwater DIC (1779 ± 40 μM) and TA (1754 ± 35 μM) inputs were depleted relative to Station ALOHA and Black Point (Table 1). Wailupe SGD delivered 16000 mol d^{-1} of DIC and 16000 mol d^{-1} of TA.

In situ coastal carbonate chemistry

Changes in DIC and TA in coastal water generally corresponded with changes in salinity, tide, and $\delta^{13}C$–DIC values at Black Point and Wailupe (Fig. 4). Ranges in DIC (1782–2779 μM) and TA (2257–2803 μM) were greatest at site 1 at Black Point (Table 2). At Wailupe, ranges in DIC were greatest at site 6 (1900–2036 μM), while the greatest range in TA occurred at site 4 (2001–2239 μM) (Table 3). In situ pH_T at Black Point was temporally and spatially variable, with the greatest range at site 1 (7.46–8.24) and the smallest range at site 3 (7.66–8.20). At Wailupe, in situ pH_T variability was comparable across all sites, ranging from 7.90 to 8.12. Mean $\Omega_{aragonite}$ was lowest and pCO_2 was highest at the nearshore sites at both study locations, with a clear spatial gradient.

Salinity normalized coastal carbonate chemistry

Diel trends in nDIC and nTA were apparent at Black Point, with minima during the day and maxima at night (Fig. 5). At Wailupe, diel trends in nDIC and nTA were less apparent (Fig. 5). Instead, nDIC and nTA generally increased at low tide when salinity was lowest at Wailupe. Ranges in nDIC and nTA were greatest at site 1 at Black Point (Table 2). At Wailupe, site 4 showed the greatest range in nDIC and nTA (Table 3). Generally, peak nDIC and nTA concentrations and minimum $\Delta n\delta^{13}C$–DIC values occurred immediately prior to sunrise at Black Point. Wailupe peak nDIC and nTA concentrations occurred around 21:00 and 06:00. Variability in nDIC was 35% greater at Black Point (1756–2423 μM) compared to Wailupe (1895–2130 μM). Similarly, nTA variability was 58% greater at Black Point (2232–2547 μM) compared to Wailupe (2275–2460 μM).

Groundwater effects on in situ coastal carbonate chemistry

The effects of SGD on coastal carbonate chemistry were calculated as residuals for DIC, TA, pH_T, pCO_2, and $\Omega_{aragonite}$ by taking the difference between in situ and salinity normalized values (Tables 2, 3). SGD accounted for positive residuals in DIC and TA of 7 to 822 μM and 4 to 452 μM at Black Point, respectively. At Wailupe, SGD accounted for negative residuals in DIC and TA of 4 to 233 μM and 17 to 460 μM, respectively. High salinity samples (34.1–34.9, $n = 9$) from Black Point were also influenced by SGD, with DIC residuals of 7 to 38 μM ($\bar{x} = 24 \pm 10$ μM) and TA residuals of 4 to 24 μM ($\bar{x} = 15 \pm 6$ μM). SGD at Wailupe lowered DIC and TA in high salinity samples (33.9–34.1, $n = 5$) by 4 to 10 μM ($\bar{x} = 7 \pm 3$ μM) and 17 to 21 μM ($\bar{x} = 18 \pm 1$ μM), respectively. Brackish water samples (27.9–32.9, $n = 12$) received, on average, 149 ± 52 μM of DIC and 95 ± 31 μM of TA from SGD at Black Point. Wailupe SGD lowered brackish water samples (28.1–33.8, $n = 8$) DIC and TA concentrations by 21 ± 15 μM and 57 ± 33 μM, respectively. We observed mean declines in pH_T from groundwater inputs of 0.02 to 0.14 units across sites at Black Point, with an overall decline of 0.00 to 0.44 units (Table 2). Groundwater-induced changes in pH_T at Wailupe lowered in situ pH_T on average by 0.00 to 0.04 units at all sites, with a range of 0.00 to 0.12 units (Table 3). SGD lowered $\Omega_{aragonite}$ on average by 0.1 to 1.0 units across all sites at Black Point and Wailupe. pCO_2 residuals from SGD ranged from 0 μatm to 1630 μatm at Black Point and 0 μatm to 220 μatm at Wailupe.

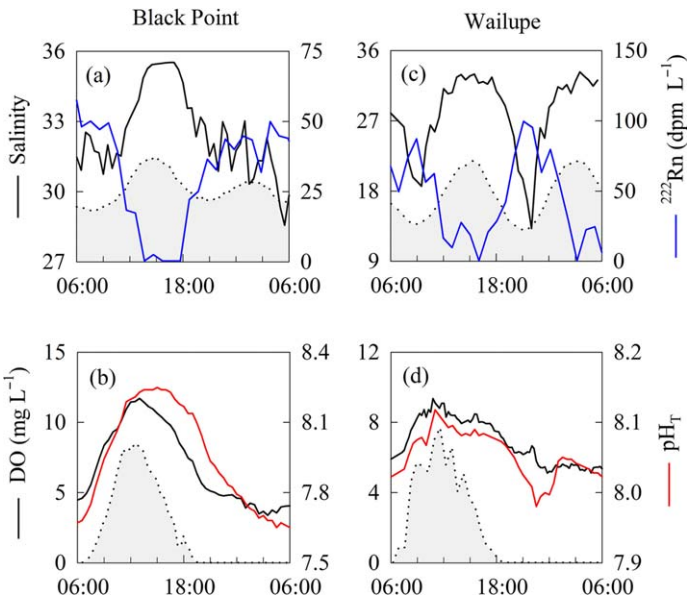

Fig. 3. Long-term time series data for the time periods that correspond to the 24-h sampling events at Black Point (12 August 2015) and Wailupe (27 September 2015). Salinity and coastal ^{222}Rn in water data are shown for (**a**) Black Point and (**c**) Wailupe. Dissolved oxygen (DO) and pH_T data are shown for (**b**) Black Point and (**d**) Wailupe. Tide (**a, c**) and PAR (**b, d**) are indicated by the shaded gray regions.

NCC and NCP rates

NCP_{daily} rates indicated a spatial progression from net respiration at site 1 (-41.3 ± 7.2 mmol C m^{-2} d^{-1}) and site 2 (-17.8 ± 11.6 mmol C m^{-2} d^{-1}) to net photosynthesis at site 3 (6.6 ± 12.7 mmol C m^{-2} d^{-1}) (Table 4). NCP_{day} rates at sites 1 and 2 were counterbalanced by more negative NCP_{night} rates, leading to net respiring conditions. The NCC_{night} rate at site 1 was greater than NCC_{day}, resulting in net dissolution at a rate of -12.9 ± 1.4 mmol $CaCO_3$ m^{-2} d^{-1}. In

Table 1. SGD endmember composition at Black Point ($n = 9$) and Wailupe ($n = 6$). Data used for the marine endmember, Station ALOHA ($n = 4$), is also displayed. The standard deviation about the mean of measurements made over the 24-h sampling periods are included. Standard deviations for Station ALOHA were calculated for measurements from 2012 to 2014.

	Black Point$_{sgd}$		Wailupe$_{sgd}$		Station ALOHA
Parameter	**Mean**	**Range**	**Mean**	**Range**	**Mean**
Salinity	4.9 ± 0.2	4.7–5.2	2.0 ± 0.5	1.3–2.5	35.2
Water temp. (°C)	24.7 ± 0.3	24.1–24.9	22.9 ± 1.2	21.9–24.9	-
^{222}Rn (dpm L^{-1})	490 ± 60	260–500	121 ± 8	96–158	-
NO_3^- (μM)	163 ± 1	162–165	71 ± 6	59–76	0.03
PO_4^{3-} (μM)	3.7 ± 0.1	3.7–3.8	1.7 ± 0.1	1.6–1.9	0.2
SiO_4^{4-} (μM)	740 ± 13	710–750	810 ± 52	730–890	1.2
NH_4^+ (μM)	0.15 ± 0.06	0.06–0.25	0.18 ± 0.03	0.16–0.20	-
DIC (μM)	3038 ± 6	3032–3046	1779 ± 40	1734–1842	2003 ± 8
TA (μM)	2946 ± 8	2937–2958	1754 ± 35	1716–1809	2323 ± 5
pH_T	7.39 ± 0.02	7.36–7.44	7.58 ± 0.03	7.54–7.62	8.06 ± 0.01
$\Omega_{aragonite}$	0.53 ± 0.04	0.48–0.59	0.35 ± 0.02	0.33–0.38	-
pCO_2 (μatm)	4000 ± 220	3600–4400	1600 ± 320	1400–1790	-
δ^{13}C-DIC (‰)	−13.6 ± 0.2	−13.8 to −13.3	−15.1 ± 0.4	−16.4 to −15.1	-

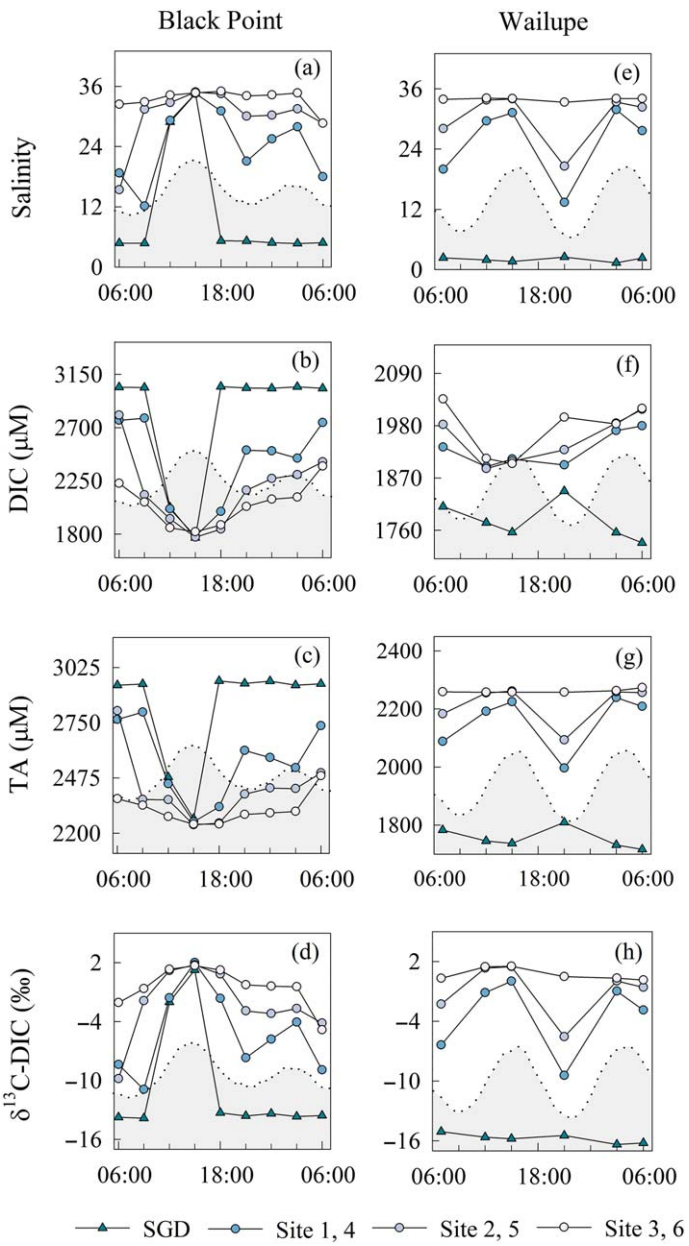

Fig. 4. Time series data from the 24-h sampling events at (**a–d**) Black Point (12 August 2015) and (**e–h**) Wailupe (27 September 2015) showing changes with time in (**a, e**) salinity, (**b, f**) DIC, (**c, g**) TA, and (**d, h**) δ^{13}C–DIC values. Tide is shown as the shaded gray region.

comparison, sites 2 and 3 were net calcifying with NCC_{daily} rates between 12.2 ± 2.1 mmol $CaCO_3$ m^{-2} d^{-1} and 51.8 ± 2.2 mmol $CaCO_3$ m^{-2} d^{-1}, respectively.

At Wailupe, there was a spatial progression from net photosynthesis and dissolution at site 4 to net photosynthesis and calcification at sites 5 and 6 (Table 4). NCP_{day} and NCP_{night} rates were similar in magnitude across all sites, ranging from 1.2 ± 0.2 to 1.5 ± 0.2 mmol C m^{-2} h^{-1} and -1.2 ± 0.3 to -0.8 ± 0.2 mmol C m^{-2} h^{-1}, respectively. NCC_{daily} rates indicated net dissolution at site 4 (-9.7 ± 0.8 mmol $CaCO_3$ m^{-2} d^{-1}) and net calcification at site 5 (6.2 ± 0.6 mmol $CaCO_3$ m^{-2} d^{-1}) and site 6 (14.7 ± 0.7 mmol $CaCO_3$ m^{-2} d^{-1}). Minimum NCC rates occurred around 21:00 at sites 4 and 5, as evidenced by changes in ΔnTA (Fig. 6).

Discussion

Results obtained from this study indicate several methodological and biogeochemical consequences of SGD into coral reef ecosystems. Groundwater-derived DIC and TA comprised large fractions of in situ coastal water DIC and TA reservoirs, and observed changes in coastal DIC and TA reservoirs due to SGD were frequently greater than changes due to biological processes. Failure to quantify groundwater-derived constituent fractions, when they are present, can bias interpretations of reef biogeochemistry toward over-attribution of changes due to biological processes.

Methodological impacts of submarine groundwater discharge on in situ coastal carbonate chemistry

The spatial and temporal variability of groundwater-induced changes in nearshore marine carbonate chemistry reported herein highlights the importance of distinguishing variability due to physical mixing of groundwater with seawater from biologically-driven variability. Previous studies have reported a wide range of DIC (451–7433 μM) and TA (781–7134 μM) concentrations in groundwater emanating from tropical islands (Schopka and Derry 2012; Cyronak et al. 2013, 2014, Lantz et al. 2014; Fackrell 2016; Fackrell et al. 2016). Many of the groundwater DIC and TA concentrations reported in the above studies were similar to or greater than those measured in this study. As groundwater DIC and TA content becomes increasingly elevated relative to ambient seawater concentrations, groundwater-derived DIC and TA will account for more substantial portions of DIC and TA reservoirs in mixed salinity water. Shaw et al. (2014) compiled DIC and TA data for twenty previous studies that calculated NCC and NCP rates using changes in DIC and TA as proxies for reef metabolism. Groundwater contributions to coastal DIC and TA observed in the present study, particularly in high salinity samples, were well within many of the diel ranges in DIC and TA observed in Shaw et al. (2014). Mean daily changes in TA ranged from 0 μM to 20 μM for seven of the ten summarized studies, and mean changes in DIC were below 55 μM for six out of the seven studies reporting these values (Shaw et al. 2014). Of the studies that mentioned freshwater influence, most salinity normalized carbonate system parameters (e.g., DIC and TA) using the traditional normalization approach, which assumes a freshwater endmember of 0 μM for both DIC and TA, or did not specify freshwater endmember C parameters.

We compared the results of salinity normalization using the traditional normalization method to the non-zero

Table 2. Black Point coastal geochemistry, including in situ and salinity normalized values for DIC, TA, pH_T, pCO_2, and $\Omega_{aragonite}$. The residual difference between in situ and salinity normalized values (e.g., changes due to SGD) is represented as an asterisk (*). The standard deviation about the mean of the measurements for each constituent is also displayed.

	Site 1		Site 2		Site 3	
Black Point	**Mean**	**Range**	**Mean**	**Range**	**Mean**	**Range**
Salinity	25.4 ± 6.9	12.2–34.6	29.9 ± 5.8	15.4–34.9	33.4 ± 2.0	28.7–35.0
Water temp. (°C)	25.9 ± 2.2	24.1–30.5	27.5 ± 1.5	25.9–29.8	27.5 ± 0.9	26.6–29.0
NO_3^- (μM)	52 ± 38	1.4–121	29 ± 40	0.9–131	7.5 ± 11	0.3–34
PO_4^{3-} (μM)	1.4 ± 0.9	0.2–2.8	0.6 ± 0.5	0.2–1.9	0.2 ± 0.2	0.1–0.8
SiO_4^{4-} (μM)	243 ± 177	14–566	116 ± 140	8.2–470	36 ± 43	3–137
NH_4^+ (μM)	1.0 ± 0.3	0.6–1.4	0.8 ± 0.3	0.4–1.6	0.4 ± 0.1	0.2–0.5
DIC (μM)	2392 ± 373	1782–2779	2182 ± 318	1775–2806	2052 ± 182	1819–2374
nDIC (μM)	2070 ± 261	1756–2423	2033 ± 205	1760–2341	1996 ± 143	1798–2191
*DIC (μM)	321 ± 228	25–822	149 ± 132	15–465	55 ± 55	7–183
TA (μM)	2561 ± 192	2257–2803	2420 ± 168	2242–2809	2318 ± 74	2244–2486
nTA (μM)	2363 ± 101	2235–2547	2326 ± 92	2234–2537	2282 ± 38	2232–2359
*TA (μM)	198 ± 130	14–452	94 ± 78	8–273	37 ± 38	4–127
pH_T	7.78 ± 0.32	7.46–8.24	7.90 ± 0.27	7.52–8.24	7.93 ± 0.21	7.66–8.20
npH_T	7.92 ± 0.29	7.58–8.34	7.96 ± 0.22	7.70–8.26	7.95 ± 0.19	7.72–8.22
$*pH_T$	−0.14 ± 0.12	−0.44 to −0.01	−0.06 ± 0.07	−0.24 to −0.01	−0.02 ± 0.02	−0.06–0.00
pCO_2 (μatm)	1360 ± 910	210–2580	860 ± 700	220–2360	640 ± 370	240–1290
$npCO_2$ (μatm)	740 ± 520	160–1450	590 ± 340	210–1050	570 ± 290	230–990
$*pCO_2$ (μatm)	620 ± 560	10–1630	270 ± 450	10–1430	70 ± 100	0–300
$\Omega_{aragonite}$	2.5 ± 1.9	0.9–5.3	3.0 ± 1.6	1.0–5.2	3.2 ± 1.2	1.8–4.8
$n\Omega_{aragonite}$	3.5 ± 1.8	1.6–6.3	3.4 ± 1.4	1.9–5.4	3.3 ± 1.1	2.1–4.9
$*\Omega_{aragonite}$	−1.0 ± 1.0	−3.5 to −0.1	−0.4 ± 0.5	−1.6 to −0.1	−0.1 ± 0.1	−0.4 to −0.1

endmember method, which takes into consideration freshwater endmember DIC and TA concentrations, for our carbonate chemistry data at both study locations. Black Point nDIC concentrations were consistently overestimated using the traditional normalization method, ranging from a mean excess of 80 ± 19 μM at a salinity range of 34 to 34.5 ($n = 5$) to a mean excess of 496 ± 206 μM at a salinity range of 28 to 34 ($n = 12$). nTA concentrations showed similar discrepancies, with mean excesses of 75 ± 19 μM at a salinity range of 34 to 34.5 ($n = 5$) and 473 ± 197 μM at a salinity range of 28 to 34 ($n = 12$). Wailupe nDIC concentrations were overestimated on average by 59 ± 1.8 μM at a salinity range of 34 to 34.5 ($n = 4$) and 176 ± 129 μM at a salinity range of 28 to 34 ($n = 10$). Excess nTA contributions from the traditional normalization method were nearly identical to nDIC estimates at Wailupe. Changes in nDIC and nTA of this magnitude will result in over- or under-estimation of NCC and NCP rates without proper salinity normalization of carbonate system parameters.

Drivers of reef metabolism

NCC

Daily NCC rates indicated net dissolution at sites closest to the groundwater springs at both study locations (Table 4). Multiple environmental stressors brought on by SGD may act synergistically to drive dissolution and reduce calcification. Seawater geochemical parameters, such as salinity, temperature, inorganic nutrient content, pH, and $\Omega_{aragonite}$, which are known to affect calcifying organisms (Fabricius 2005; Fabry et al. 2008; Doney et al. 2009; Ries et al. 2009), were largely a function of SGD at our study locations (Tables 2, 3). While difficult to constrain in our study since many of these geochemical parameters co-varied and/or were calculated based on dependent variables, their potential effects on NCC are discussed below.

Cool, low salinity water has been shown to stress corals and exceed calcifying organisms' physical thresholds (Coles and Jokiel 1992; Jokiel et al. 1993; Lough and Barnes 2000; Fabricius 2005). Similarly, low pH and $\Omega_{aragonite}$ conditions can support elevated bioerosion rates (Wisshak et al. 2012; Crook et al. 2013; Barkley et al. 2015; Silbiger et al. 2016) and enhance dissolution of $CaCO_3$ sediments (Cyronak et al. 2013; Cyronak and Eyre 2016). Bioeroders are currently regarded as one of the primary drivers of reef erosion (Andersson and Gledhill 2013) and may play an important role in the dissolution of Maunalua Bay reefs. Low salinity, pH, and $\Omega_{aragonite}$ conditions generally coincided with periods of net dissolution at both study locations (Figs. 3, 5,

Table 3. Wailupe coastal geochemistry, including in situ and salinity normalized values for DIC, TA, pH_T, pCO_2, and $\Omega_{aragonite}$. The residual difference between in situ and salinity normalized values (e.g., changes due to SGD) is represented as an asterisk (*). The standard deviation about the mean of the measurements for each constituent is also displayed.

	Site 4		Site 5		Site 6	
Wailupe	**Mean**	**Range**	**Mean**	**Range**	**Mean**	**Range**
Salinity	25.6 ± 7.4	13.4–31.8	30.4 ± 5.3	20.6–34.0	33.9 ± 0.3	33.3–34.1
Water temp. (°C)	25.8 ± 1.4	24.6–27.7	26.6 ± 1.6	24.5–28.4	26.9 ± 1.4	25.5–28.6
NO_3^- (μM)	15 ± 14	4.0–40	5.9 ± 9.4	0.3–24	0.2 ± 0.1	0.2–0.3
PO_4^{3-} (µM)	0.8 ± 0.4	0.3–1.4	0.4 ± 0.3	0.2–1.0	0.1 ± 0.1	0.1–0.2
SiO_4^{4-} (μM)	199 ± 168	45–473	89 ± 130	6–333	6 ± 5	2–15
NH_4^+ (μM)	0.3 ± 0.2	0.1–0.5	0.6 ± 0.1	0.4–0.8	0.5 ± 0.3	0.3–1.2
DIC (μM)	1931 ± 37	1894–1980	1951 ± 50	1890–2014	1974 ± 56	1900–2036
nDIC (μM)	2013 ± 83	1917–2130	1988 ± 69	1895–2050	1982 ± 59	1905–2047
*DIC (μM)	−82 ± 86	−233 to −18	−37 ± 45	−120 to −5	−8 ± 3	−13 to −4
TA (μM)	2159 ± 94	2001–2239	2218 ± 68	2093–2261	2261 ± 6	2258–2273
nTA (μM)	2339 ± 69	2280–2460	2302 ± 30	2277–2360	2282 ± 7	2275–2292
*TA (μM)	−180 ± 160	−460 to −55	−84 ± 97	−267 to −19	−20 ± 5	−30 to −17
pH_T	8.02 ± 0.08	7.90–8.12	8.02 ± 0.08	7.94–8.12	8.01 ± 0.07	7.92–8.10
npH_T	8.06 ± 0.04	8.02–8.13	8.03 ± 0.07	7.95–8.12	8.01 ± 0.07	7.92–8.10
$*pH_T$	−0.04 ± 0.05	−0.12 to −0.01	−0.01 ± 0.02	−0.06 to 0.00	0.00 ± 0.00	0.00–0.00
pCO_2 (μatm)	460 ± 130	330–670	440 ± 96	310–540	440 ± 90	330–560
$npCO_2$ (μatm)	390 ± 60	310–450	420 ± 80	310–520	440 ± 90	330–560
$*pCO_2$ (μatm)	70 ± 80	10–220	20 ± 40	0–100	0 ± 0	0–0
$\Omega_{aragonite}$	2.7 ± 0.9	1.4–3.6	3.1 ± 0.9	2.1–4.2	3.3 ± 0.6	2.6–4.1
$n\Omega_{aragonite}$	3.7 ± 0.3	3.4–4.1	3.6 ± 0.6	3.0–4.3	3.4 ± 0.6	2.7–4.2
$*\Omega_{aragonite}$	−1.0 ± 0.9	−2.5 to −0.3	−0.5 ± 0.6	−1.6 to −0.1	−0.1 ± 0.0	−0.1 to −0.1

6). Minima in $\Omega_{aragonite}$ at Black Point and Wailupe were similar to and even lower (0.90 units) than previously recorded minimum values (1.13 units) in similar reef studies (summarized by Shaw et al. 2012). These low $\Omega_{aragonite}$ values and coincident respiring conditions at the nearshore sites at both study locations could support dissolution of carbonate materials in underlying pore waters and reef microenvironments (Andersson and Gledhill 2013). Further, in algal dominated reefs such as Black Point and Wailupe, the release of labile dissolved organic C by algae can enhance microbial overgrowth on proximal corals, leading to mortality (Smith et al. 2006). Live coral cover was lowest at the nearshore sites, where exposure to groundwater was greatest. Crook et al. (2013) observed similar trends in benthic cover as a function of SGD exposure in Puerto Morelos, Mexico. Since NCC reflects the net balance between calcification and dissolution, this disparity in benthic cover could lead to lower calcification rates relative to the offshore sites, allowing dissolution to dominate at the sites closest to groundwater sources.

NCP

At both locations, autotrophic utilization of nDIC reached daily maxima midday when PAR peaked, while respiration drove nDIC production at night (Fig. 6). Typically, photosynthesis and respiration on reefs offset each other, resulting in near-zero daily integrated NCP rates (Kinsey 1985). For reefs with significant geochemical variability from SGD, this relationship may shift. At Black Point, respiration dominated over photosynthesis at sites 1 and 2, resulting in NCP_{daily} rates of -41.3 ± 7.2 and -17.8 ± 11.6 mmol C m^{-2} d^{-1}, respectively. Net respiration has been observed in other reefs in and beyond Hawai'i (Shamberger et al. 2011; Muehllehner et al. 2016) as well as those experiencing inputs from wastewater (Smith et al. 1981; Kinsey 1985). Reef microbialization is closely associated with increasing algal dominance and anthropogenic stressors, such as nutrient pollution (Haas et al. 2016). Groundwater discharge at Black Point is composed of a substantial fraction of wastewater from proximal cesspools (Richardson et al. in press). The delivery of C, N, and P from cesspools via SGD could fuel the net heterotrophic conditions at sites 1 and 2 at Black Point, and contribute to the elevation in ΔnDIC values and NCP rates observed at all Black Point sites relative to Wailupe (Fig. 6). Nearly all site-specific mean NO_3^-, PO_4^{3-}, and SiO_4^{4-} concentrations at Black Point were elevated relative to ambient seawater (Table 2), and Richardson et al. (in press) previously observed large deviations from

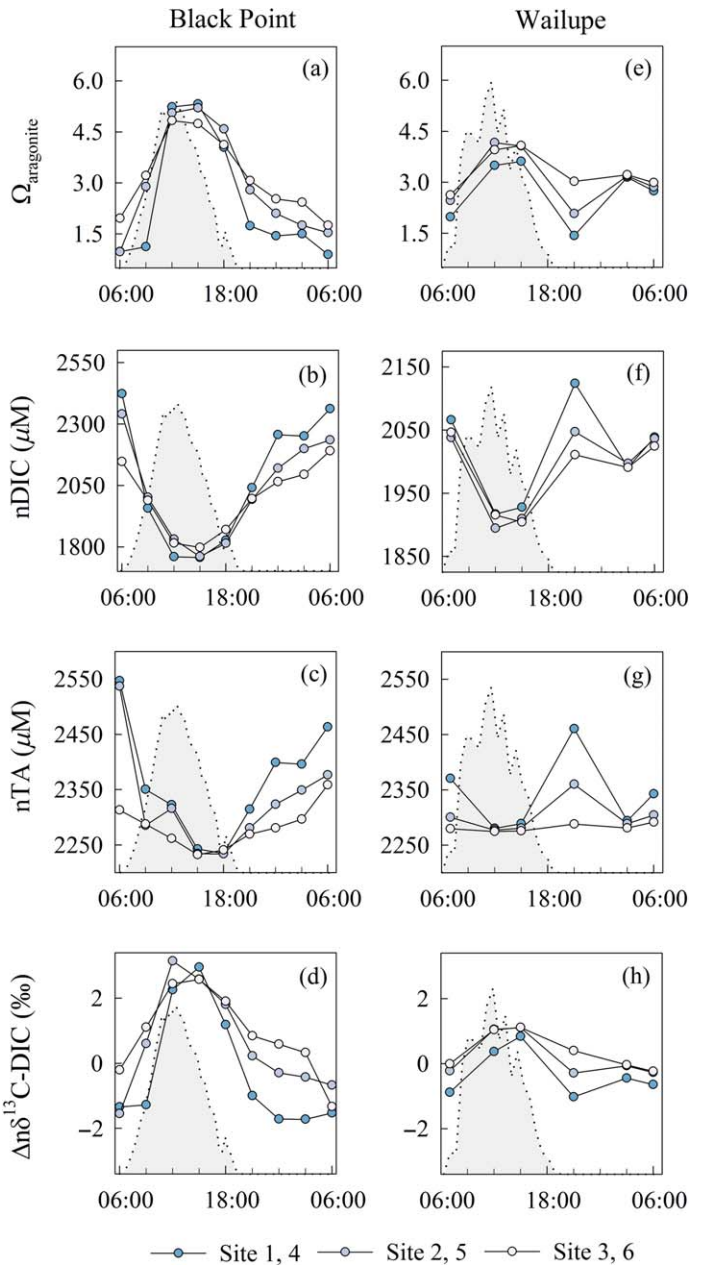

Fig. 5. Time series data from the 24-h sampling events at (**a–d**) Black Point (12 August 2015) and (**e–h**) Wailupe (27 September 2015) showing changes with time in (**a, e**) $\Omega_{aragonite}$, (**b, f**) nDIC, (**c, g**) nTA, and (**d, h**) $\Delta n\delta^{13}$C–DIC values. PAR is shown as the shaded gray region.

conservative mixing lines between salinity and NO_3^-, NH_4^+, and SiO_4^{4-} at Black Point. The widespread ranges in ΔnDIC and inorganic nutrient concentrations observed in this study across all sites at Black Point, along with the previously observed negative residuals in NO_3^- and SiO_4^{4-} concentrations relative to conservative mixing trends, provide evidence that inorganic nutrient inputs from SGD at Black Point may enhance photosynthesis and subsequent respiration. Remineralization of organic matter has been shown to drive pH decline in other coastal ecosystems receiving nutrient inputs on the same order of magnitude observed here, once SGD has been accounted for (Sunda and Cai 2012; Wallace et al. 2014).

Additionally, SGD at both sites is oxic (Richardson et al. in press). If peak groundwater discharge occurs at night when respiration has driven DO levels below groundwater endmember DO concentrations, then groundwater will act as a source of DO to surrounding seawater, potentially enabling more efficient respiration than would occur under lower DO conditions. The changes in ΔnDIC and $\Delta n\delta^{13}$C-DIC values from 21:00 to 03:00 at the nearshore sites at Wailupe may reflect enhancement of respiration and also help explain the increase in ΔnTA values at 21:00 (Fig. 6). Respiration of organic C introduces CO_2 into the water column, which can increase dissolution of $CaCO_3$ via localized acidification. Groundwater discharge at Wailupe did elevate DO levels around 21:00 as evidenced by the difference between in situ DO and salinity normalized DO (Fig. 7).

While it is possible that the changes in nDIC and nTA (and subsequently, ΔnDIC and ΔnTA) at low tide at Wailupe were an artifact of salinity normalization, we found little evidence in support of this hypothesis. Groundwater DIC and TA content varied by approximately 100 μM at Wailupe. To account for this variability, we salinity normalized Wailupe carbonate chemistry data using both a mean and time-specific groundwater endmember to examine if trends in nDIC and nTA were consistent between the two approaches. While the magnitude of changes in nDIC and nTA shifted, the maxima in ΔnDIC and ΔnTA at 21:00 remained. Because Wailupe groundwater DIC and TA content changed predictably ($TA = 0.87 \cdot DIC + 211.56$, $R^2 = 0.99$), likely as a result of tidal mixing with biogeochemically-altered seawater, we were able to use this relationship to predict a series of DIC and TA values for SGD at 21:00 to see if any groundwater DIC and TA endmembers could remove the observed trend. Our sensitivity analysis found that no endmember consistent with the SGD geochemistry observed at Wailupe could remove the nTA trends while maintaining a reasonable trend in nDIC (e.g., peaks in NCP coincident with PAR). While salinity normalization can account for the direct physical effects of SGD in reef systems, it cannot account for the indirect biological consequences of these inputs. Distinguishing between the two processes is complicated in systems with a transient groundwater endmember.

Salinity normalized δ^{13}C–DIC values corroborate reef metabolism trends

Photosynthetic organisms preferentially take up DIC containing the lighter stable isotope of C (^{12}C), leading to an increase in δ^{13}C–DIC values in the residual DIC pool. As heterotrophs remineralize the ^{13}C-depleted organic matter produced by photosynthesizers, DIC with low δ^{13}C–DIC values is reintroduced into the DIC pool. In contrast, calcification

Table 4. Hourly and daily NCC and NCP rates for each site. Hourly rates were split into daytime ("day") and nighttime ("night") periods. Daytime was defined as 09:00 to 18:00, while nighttime extended from 18:00 to 06:00. NCC and NCP rates are presented with uncertainties, which were determined by propagating errors on ΔnTA, ΔnDIC, water depth, and air-sea CO_2 fluxes through all associated calculations.

	NCC_{day}	NCC_{night}	NCP_{day}	NCP_{night}	NCC_{daily}	NCP_{daily}
	(mmol $CaCO_3$ m^{-2} h^{-1})		(mmol C m^{-2} h^{-1})		(mmol $CaCO_3$ m^{-2} d^{-1})	(mmol C m^{-2} d^{-1})
Black Point						
Site 1	0.8 ± 0.1	−1.9 ± 0.1	7.1 ± 0.5	−10.5 ± 0.4	−12.9 ± 1.4	−41.3 ± 7.2
Site 2	2.2 ± 0.1	−1.1 ± 0.1	9.6 ± 0.7	−11.1 ± 0.6	12.2 ± 2.1	–17.8 ± 11.6
Site 3	3.1 ± 0.1	1.2 ± 0.1	9.3 ± 0.8	−8.8 ± 0.7	51.8 ± 2.2	6.6 ± 12.7
Wailupe						
Site 4	0.1 ± 0.1	−0.9 ± 0.1	1.3 ± 0.2	−1.2 ± 0.3	−9.7 ± 0.8	0.6 ± 3.8
Site 5	0.5 ± 0.1	0.1 ± 0.1	1.5 ± 0.2	−0.8 ± 0.2	6.2 ± 0.6	8.0 ± 3.1
Site 6	0.7 ± 0.1	0.6 ± 0.1	1.2 ± 0.2	−0.8 ± 0.2	14.7 ± 0.7	4.6 ± 3.0

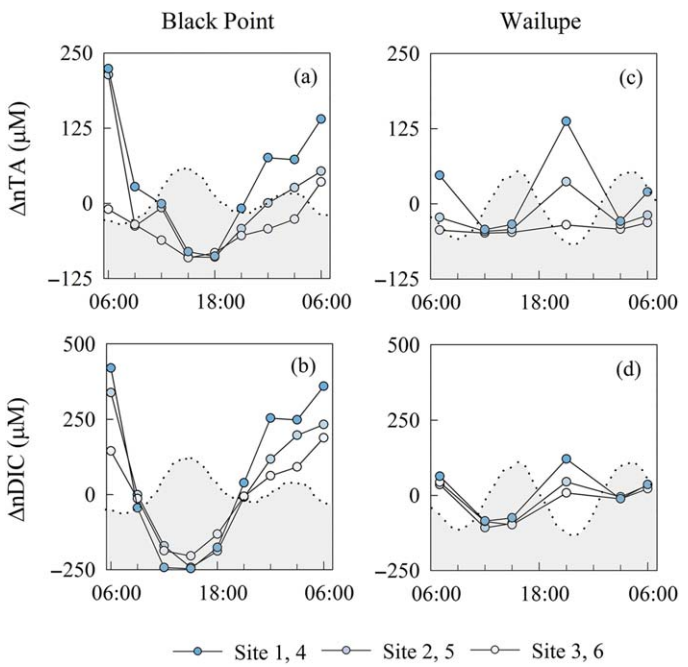

Fig. 6. Time series ΔnTA and ΔnDIC values are shown for (**a, b**) Black Point and (**c, d**) Wailupe.

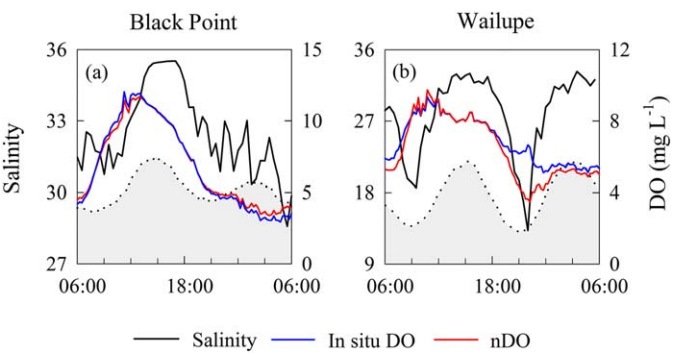

Fig. 7. Comparison of in situ dissolved oxygen (DO) and salinity normalized dissolved oxygen (nDO) concentrations at (**a**) Black Point and (**b**) Wailupe.

and dissolution do not fractionate DIC substantially (Smith and Kroopnick 1981; Zeebe and Wolf-Gladrow 2001). As such, the $\Delta n\delta^{13}C$–DIC values reported herein are primarily a function of changes in $^{13}C/^{12}C$ ratios from DIC generated and utilized by respiration and photosynthesis, respectively.

At Black Point, the mean $\Delta n\delta^{13}C$–DIC value (–0.1 ± 1.9‰) and consistently lower $\Delta n\delta^{13}C$–DIC values observed at site 1 relative to the other sites were in line with the previously discussed NCP calculations, which indicated net heterotrophy. Respiration will drive $n\delta^{13}C$–DIC values below bulk ocean stable C isotopic values typical of open ocean conditions around Hawai'i (1.2‰ at Station ALOHA) (Brix et al. 2004). In contrast, mean $\Delta n\delta^{13}C$–DIC values from sites 2 and 3 at Black Point were 0.8 ± 1.5‰ and 1.1 ± 1.1‰, respectively. These shifts in mean $^{13}C/^{12}C$ ratios, from low (site 1) to high (site 3) relative to bulk ocean $\delta^{13}C$–DIC values, corroborate the observed change in NCP rates from net heterotrophy to net autotrophy at Black Point. $\Delta n\delta^{13}C$–DIC values at Wailupe generally followed NCP trends as well, although mean $\Delta n\delta^{13}C$-DIC values were smaller in magnitude across all sites (−0.3 ± 0.6‰–0.5 ± 0.5‰) relative to Black Point. Differences in the magnitude of $\Delta n\delta^{13}C$–DIC values between study locations also substantiate our NCP calculations, which showed that respiration and photosynthesis were elevated at Black Point compared to Wailupe (Fig. 5). As respiration and photosynthesis increase in magnitude, a greater fraction of the DIC pool is influenced by these biological processes, shifting $n\delta^{13}C$–DIC values away from open ocean stable C isotopic values.

We also calculated enrichment factors using $\Delta n\delta^{13}C$–DIC values from both study locations to determine if observed enrichment factors align with those previously reported for

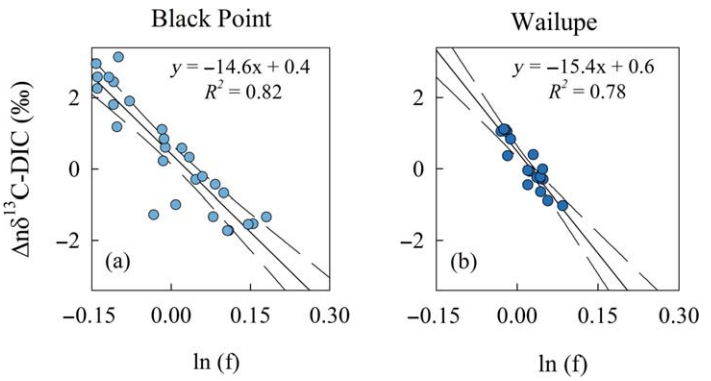

Fig. 8. Relationship between the natural log of the fraction (*f*) of nDIC relative to marine endmember DIC, and $\Delta n\delta^{13}C$–DIC values for (**a**) Black Point and (**b**) Wailupe, with 95% confidence intervals for the regressions shown as dashed lines.

coral reefs. Enrichment factors quantitatively express the tendency of biological and physical processes to discriminate against specific stable isotopes of a substrate material. In the case of DIC used and produced by biological processes in reefs, enrichment factors should reflect the occurrence of photosynthesis. Enrichment factors were calculated using the following equation:

$$\varepsilon = \Delta\delta_x / \ln(f) \quad (7)$$

where ε is the enrichment factor, $\Delta\delta_x$ is the change between the marine endmember $\delta^{13}C$–DIC value and measured $\Delta n\delta^{13}C$–DIC value, and f is the ratio of the measured nDIC to marine endmember DIC. Enrichment factors appear as the slope of the line on a plot of $\Delta n\delta^{13}C$–DIC values vs. ln (*f*). Enrichment factors at Black Point (–14.6‰) and Wailupe (–15.4‰) were within the range of values (–14‰ to −18‰) commonly observed in reefs (Fig. 8) (Land et al. 1975; Smith and Kroopnick 1981). The consistency of these values with previous studies corroborates our use of $\Delta n\delta^{13}C$–DIC values as a proxy for C cycling.

Limitations

The cumulative effect of SGD on nearshore carbonate chemistry at both locations was site dependent as salinity ranges, exposure to physicochemical parameters, and mixing dynamics were not comparable between sites. Because of these differences, comparison between the two study locations was difficult. Additionally, differences in benthic composition between study locations, as well as between individual sampling sites within these locations, complicated the assessment of biological effects on carbonate system parameters. While we observed intriguing trends in NCC and NCP rates with respect to groundwater discharge variability and exposure, future studies that assess the long-term variability of these processes will be of great value, as we only presented data from two 24-h sampling events. The 24-h sampling events can be put into context of long-term trends by examining SGD over the month-long monitoring performed at each site (Fig. 2). At Black Point, the 24-h sampling represented a low-flow period in a relatively dry month followed by rain events that increased SGD. At Wailupe, the 24-h sampling period was performed during above average SGD conditions. The NCC and NCP calculations also used mean water depth and residence times, parameters which we know vary in time and space. Admittedly, our use of a mean residence time for all sites oversimplified these complex systems.

Conclusions

We measured month-long and 24-h changes in groundwater flux as well as geochemical and carbonate system parameters across salinity gradients in two contrasting groundwater-influenced reefs along the southeastern coast of O'ahu. SGD into these reef systems accounted for up to 30% and 16% of coastal DIC and TA reservoirs, respectively. Groundwater inorganic C loadings were spatially heterogeneous at our two study areas, thus highlighting the need for high-resolution groundwater endmember data in future studies. Salinity normalized carbonate system parameters revealed spatial trends in reef metabolism at both sites, generally resulting in an increase in NCP and NCC rates as exposure to groundwater decreased, although community responses to environmental variables were location specific. Overall, high groundwater exposure sites showed low daytime calcification rates and elevated dissolution rates at night relative to low groundwater exposure sites at both reefs. To our knowledge, this study is the first to comprehensively evaluate a suite of carbonate system parameters and to separately attribute their variability to both SGD and biological processes. As freshwater discharge occurs in many coral reef ecosystems, either as riverine or groundwater inputs, salinity normalization with adequately characterized endmembers must become standard for studies of the biogeochemistry of these locations. The ability of groundwater to modify and drive coastal carbonate chemistry in reefs is spatially and temporally variable. Future efforts should address the long-term variability of SGD material fluxes and their role in reef metabolism in nearshore reef systems with varying levels of groundwater exposure.

References

Amato, D. W. 2015. Ecophysiological responses of macroalgae to submarine groundwater discharge in Hawai'i. Ph.D. thesis. Univ. of Hawai'i at Mānoa.

Andersson, A. J., and D. Gledhill. 2013. Ocean acidification and coral reefs: Effects on breakdown, dissolution, and net ecosystem calcification. Ann. Rev. Mar. Sci. **5**: 321–348. doi:10.1146/annurev-marine-121211-172241

Barkley, H. C., A. L. Cohen, Y. Golbuu, V. R. Starczak, T. M. DeCarlo, and K. E. Shamberger. 2015. Changes in coral

reef communities across a natural gradient in seawater pH. Sci. Adv. **1**: E1500328. doi:10.1126/sciadv.1500328

Blanco, A. C., A. Watanabe, K. Nadaoka, S. Motooka, E. C. Herrera, and T. Yamamoto. 2011. Estimation of nearshore groundwater discharge and its potential effects on a fringing coral reef. Mar. Poll. Bull. **62**: 770–785. doi:10.1016/j.marpolbul.2011.01.005

Borges, A. V., J. P. Vanderborght, L. S. Schiettecatte, F. Gazeau, S. Ferrón-Smith, B. Delille, and M. Frankignoulle. 2004. Variability of the gas transfer velocity of CO_2 in a macrotidal estuary (the Scheldt). Estuaries **27**: 593–603. doi:10.1007/BF02907647

Brix, H., N. Gruber, and C. D. Keeling. 2004. Interannual variability of the upper ocean carbon cycle at station ALOHA near Hawai'i. Global Biogeochem. Cycles **18**: GB4019. doi:10.1029/2004GB002245

Cardenas, M. B., and others. 2010. Linking regional sources and pathways for submarine groundwater discharge at a reef by electrical resistivity tomography, ^{222}Rn, and salinity measurements. Geophys. Res. Lett. **37**: L16401. doi:10.1029/2010GL044066

Coles, S. L., and P. L. Jokiel. 1992. Effects of salinity on coral reefs, p. 147–166. *In* D. W. Connell and D. W. Hawker [eds.], Pollution in tropical aquatic systems. CRC Press.

Crook, E. D., D. Potts, M. Rebolledo-Vieyra, L. Hernandez, and A. Paytan. 2012. Calcifying coral abundance near low-pH springs: Implications for future ocean acidification. Coral Reefs **31**: 239–245. doi:10.1007/s00338-011-0839-y

Crook, E. D., A. L. Cohen, M. Rebolledo-Vieyra, L. Hernandez, and A. Paytan. 2013. Reduced calcification and lack of acclimatization by coral colonies growing in areas of persistent natural acidification. Proc. Natl. Acad. Sci. USA **110**: 11044–11049. doi:10.1073/pnas.1301589110

Cyronak, T., I. R. Santos, D. V. Erler, and B. D. Eyre. 2013. Groundwater and porewater as major sources of alkalinity to a fringing coral reef lagoon (Muri Lagoon, Cook Islands). Biogeosciences **10**: 2467–2480. doi: 10.5194/bg-10-2467-2013

Cyronak, T., I. R. Santos, D. V. Erler, D. T. Maher, and B. D. Eyre. 2014. Drivers of pCO_2 variability in two contrasting coral reef lagoons: The influence of submarine groundwater discharge. Global Biogeochem. Cycles **28**: 398–414. doi:10.1002/2013GB004598

Cyronak, T., and B. D. Eyre. 2016. The synergistic effects of ocean acidification and organic metabolism on calcium carbonate ($CaCO_3$) dissolution in coral reef sediments. Mar. Chem. **183**: 1–12. doi:10.1016/j.marchem.2016.05.001

Dickson, A. G., and F. J. Millero. 1987. A comparison of the equilibrium constants for the dissociation of carbonic acid in seawater media. Deep Sea Res. Part A Oceanogr. Res. Pap. **34**: 1733–1743. doi:10.1016/0198-0149(87)90021-5

Dickson, A. G., J. D. Afghan, and G. C. Anderson. 2003. Reference materials for oceanic CO_2 analysis: A method for the certification of total alkalinity. Mar. Chem. **80**: 185–197. doi:10.1016/S0304-4203(02)00133-0

Dimova, N. T., P. W. Swarzenski, H. Dulaiova, and C. R. Glenn. 2012. Utilizing multichannel electrical resistivity methods to examine the dynamics of the fresh water–seawater interface in two Hawaiian groundwater systems. J. Geophys. Res. Oceans **117**: C02012. doi:10.1029/2011JC007509

Doney, S. C., V. J. Fabry, R. A. Feely, and J. A. Kleypas. 2009. Ocean acidification: The other CO_2 problem. Ann. Rev. Mar. Sci. **1**: 169–162. doi:10.1146/annurev.marine.010908.163834

Dore, J. E., R. Lukas, D. W. Sadler, M. J. Church, and D. M. Karl. 2009. Physical and biogeochemical modulation of ocean acidification in the central North Pacific. Proc. Natl. Acad. Sci. USA **106**: 12235–12240. doi:10.1073/pnas.0906044106

Dulai, H., J. Kamenik, C. A. Waters, J. Kennedy, J. Babinec, J. Jolly, and M. Williamson. 2015. Autonomous long-term gamma-spectrometric monitoring of submarine groundwater discharge trends in Hawai'i. J. Radioanal. Nucl. Chem. **307**: 1865–1870. doi:10.1007/s10967-015-4580-9

Fabricius, K. E. 2005. Effects of terrestrial runoff on the ecology of corals and coral reefs: Review and synthesis. Mar. Poll. Bull. **50**: 125–146. doi:10.1016/j.marpolbul. 2004.11.028

Fabry, V. J., B. A. Seibel, R. A. Feely, and J. C. Orr. 2008. Impacts of ocean acidification on marine fauna and ecosystem processes. ICES J. Mar. Sci. **65**: 414–432. doi:10.1093/icesjms/fsn048

Fackrell, J. 2016. Geochemical evolution of Hawaiian groundwater. Ph.D. thesis. Univ. of Hawai'i at Mānoa.

Fackrell, J., C. Glenn, B. Popp, R. Whittier, and H. Dulai. 2016. Wastewater injection, aquifer biogeochemical reactions, and resultant groundwater N fluxes to coastal waters: Kā'anapali, Maui, Hawai'i. Mar. Poll. Bull. **110**: 281–292. doi:10.1016/j.marpolbul.2016.06.050

Ferrier-Pagès, C., J. Gattuso, S. Dallot, and J. Jaubert. 2000. Effect of nutrient enrichment on growth and photosynthesis of the zooxanthellate coral Stylophora pistillata. Coral Reefs **19**: 103–113. doi:10.1007/s003380000078

Frankignoulle, M., J. P. Gattuso, R. Biondo, I. Bourge, G. Copin-Montégut, and M. Pichon. 1996. Carbon fluxes in coral reefs. II. Eulerian study of inorganic carbon dynamics and measurement of air-sea CO_2 exchanges. Mar. Ecol. Prog. Ser. **145**: 123–132. doi:10.3354/meps145123

Friis, K., A. Körtzinger, and D. W. Wallace. 2003. The salinity normalization of marine inorganic carbon chemistry data. Geophys. Res. Lett. **30**: 1085. doi:10.1029/2002GL015898

Ganguli, P. M., P. W. Swarzenski, H. Dulaiova, C. R. Glenn, and A. R. Flegal. 2014. Mercury dynamics in a coastal aquifer: Maunalua Bay, O'ahu, Hawai'i. Estuar. Coast. Shelf Sci. **140**: 52–65. doi:10.1016/j.ecss.2014.01.012

Gran, G. 1952. Determination of the equivalence point in potentiometric titrations. Part II. Analyst **77**: 661–671. doi:10.1039/AN9527700661

Haas, A. F., and others. 2016. Global microbialization of coral reefs. Nat. Microbiol. **1**: 16042. doi:10.1038/nmicrobiol.2016.42

Johnson, H. K. 1999. Simple expressions for correcting wind speed data for elevation. Coast. Eng. **36**: 263–269. doi:10.1016/S0378-3839(99)00016-2

Jokiel, P. L., C. L. Hunter, S. Taguchi, and L. Watarai. 1993. Ecological impact of a fresh-water "reef kill" in Kaneohe Bay, O'ahu, Hawai'i. Coral Reefs **12**: 177–184. doi:10.1007/BF00334477

Kinsey, D. W. 1985. Metabolism, calcification and carbon production. I. Systems level studies: Metabolism, calcification and carbon production: 1 systems level studies, *p*. 505–526. *In* C. Gabrie and B. Salvat [Eds.], Proceedings of The Fifth International Coral Reef Congress. Tahiti.

Kwon, E. Y., and others. 2014. Global estimate of submarine groundwater discharge based on an observationally constrained radium isotope model. Geophys. Res. Lett. **41**: 8438–8444. doi:10.1002/2014GL061574

Land, L. S., J. C. Lang, and D. J. Barnes. 1975. Extension rate: A primary control on the isotopic composition of West Indian (Jamaican) scleractinian reef coral skeletons. Mar. Biol. **33**: 221–233. doi:10.1007/BF00390926

Lantz, C. A., M. J. Atkinson, C. W. Winn, and S. E. Kahng. 2014. Dissolved inorganic carbon and total alkalinity of a Hawaiian fringing reef: Chemical techniques for monitoring the effects of ocean acidification on coral reefs. Coral Reefs **33**: 105–115. doi:10.1007/s00338-013-1082-5

Lapointe, B. E., R. Langton, B. J. Bedford, A. C. Potts, O. Day, and C. Hu. 2010. Land-based nutrient enrichment of the Buccoo Reef Complex and fringing coral reefs of Tobago, West Indies. Mar. Poll. Bull. **60**: 334–343. doi:10.1016/j.marpolbul.2009.10.020

Lewis, J. B. 1987. Measurements of groundwater seepage flux onto a coral reef: Spatial and temporal variations. Limnol. Oceanogr. **32**: 1165–1169. doi:10.4319/lo.1987.32.5.1165

Lough, J. M., and D. J. Barnes. 2000. Environmental controls on growth of the massive coral Porites. J. Exp. Mar. Biol. Ecol. **245**: 225–243. doi:10.1016/S0022-0981(99)00168-9

Marubini, F. 1996. The physiological response of hermatypic corals to nutrient enrichment. Ph.D. thesis. Univ. of Glasgow.

Mehrback, C., C. H. Culberson, J. E. Hawley, and R. M. Pytkowicz. 1973. Measurement of the apparent dissociation constant of carbonic acid in seawater at atmospheric pressure. Limnol. Oceanogr. **18**: 907. doi:10.4319/lo.1973.18.6.0897.

Moore, W. S. 2000. Ages of continental shelf waters determined from ^{223}Ra and ^{224}Ra. J. Geophys. Res. **105**: 117–122. doi:10.1029/1999JC000289

Moore, W. S. 2010. The effect of submarine groundwater discharge on the ocean. Ann. Rev. Mar. Sci. **2**: 59–88. doi:10.1146/annurev-marine-120308-081019

Muehllehner, N., C. Langdon, A. Venti, and D. Kadko. 2016. Dynamics of carbonate chemistry, production, and calcification of the Florida Reef Tract (2009–2010): Evidence for seasonal dissolution. Global Biogeochem. Cycles **30**: 661–688. doi:10.1002/2015GB005327

Nelson, C., and others. 2015. Fluorescent dissolved organic matter as a multivariate biogeochemical tracer of submarine groundwater discharge in coral reef ecosystems. Mar. Chem. **177**: 232–243. doi:10.1016/j.marchem.2015.06.026

NOAA National Centers for Coastal Science (NOAA). 2003. Benthic habitat of the Hawaiian Islands. Hawai'i Statewide GIS Program. Available from http://www.state.hi.us/dbedt/gis/index.html

Paytan, A., G. G. Shellenbarger, J. H. Street, M. E. Gonneea, K. Davis, M. B. Young, and W. S. Moore. 2006. Submarine groundwater discharge: An important source of new inorganic nitrogen to coral reef ecosystems. Limnol. Oceanogr. **51**: 343–348. doi:10.4319/lo.2006.51.1.0343

Pierrot, D., E. Lewis, and D. W. Wallace. 2006. MS Excel Program Developed for CO_2 System Calculations. ORNL/CDIAC-105a. Carbon Dioxide Information Analysis Center, Oak Ridge National Laboratory, U.S. Department of Energy, Oak Ridge, Tennessee.

Raymond, P. A., and J. J. Cole. 2001. Gas exchange in rivers and estuaries: Choosing a gas transfer velocity. Estuar. Coasts **24**: 312–317. doi:10.2307/1352954

Richardson, C. M., H. Dulai, and R. B. Whittier. 2015. Sources and spatial variability of groundwater-delivered nutrients in Maunalua Bay, O'ahu, Hawai 'i. J. Hydrol. Reg. Stud. **11**: 178–193. doi:10.1016/j.ejrh.2015.11.006

Riebesell, U., V. J. Fabry, L. Hansson, and J. P. Gattuso. 2010. Guide to best practices for ocean acidification research and data reporting. Publications Office of the European Union, Luxembourg.

Ries, J. B., A. L. Cohen, and D. C. McCorkle. 2009. Marine calcifiers exhibit mixed responses to CO_2-induced ocean acidification. Geology **37**: 1131–1134. doi:10.1130/G30210A.1

Salata, G. G., L. A. Roelke, and L. A. Cifuentes. 2000. A rapid and precise method for measuring stable carbon isotope ratios of dissolved inorganic carbon. Mar. Chem. **69**: 153–161. doi:10.1016/S0304-4203(99)00102-4

Sansone, F. J., M. E. Holmes, and B. N. Popp. 1999. Methane stable isotopic ratios and concentrations as indicators of methane dynamics in estuaries. Global Biogeochem. Cycles **13**: 463–474. doi:10.1029/1999GB900012

Santos, I. R., R. N. Glud, D. Maher, D. Erler, and B. D. Eyre. 2011. Diel coral reef acidification driven by porewater advection in permeable carbonate sands, Heron Island, Great Barrier Reef. Geophys. Res. Lett. **38**: L03604. doi:10.1029/2010GL046053

Schopka, H. H., and L. A. Derry. 2012. Chemical weathering fluxes from volcanic islands and the importance of groundwater: The Hawaiian example. Earth Planet. Sci. Lett. **339**: 67–78. doi:10.1016/j.epsl.2012.05.028

Shaish, L., G. Levy, G. Katzir, and B. Rinkevich. 2010. Coral reef restoration (Bolinao, Philippines) in the face of frequent natural catastrophes. Restor. Ecol.. **18**: 285–299. doi:10.1111/j.1526-100X.2009.00647.x

Shamberger, K. E., R. A. Feely, C. L. Sabine, M. J. Atkinson, E. H. DeCarlo, F. T. Mackenzie, P. S. Drupp, and D. A.

Butterfield. 2011. Calcification and organic production on a Hawaiian coral reef. Mar. Chem. **127**: 64–75. doi: 10.1016/j.marchem.2011.08.003

Shaw, E. C., B. I. McNeil, and B. Tilbrook. 2012. Impacts of ocean acidification in naturally variable coral reef flat ecosystems. J. Geophys. Res. Oceans **117**: C03038. doi: 10.1029/2011JC007655

Shaw, E. C., S. R. Phinn, B. Tilbrook, and A. Steven. 2014. Comparability of slack water and lagrangian flow respirometry methods for community metabolic measurements. PLoS One **9**: e112161. doi:10.1371/journal. pone.0112161

Silbiger, N. J., Ò. Guadayol, F. Thomas, and M. Donahue. 2016. A novel μCT analysis reveals different responses of bioerosion and secondary accretion to environmental variability. PLoS One **11**: e0153058. doi:10.1371/journal. pone.0153058

Slomp, C. P., and P. Van Cappellen. 2004. Nutrient inputs to the coastal ocean through submarine groundwater discharge: Controls and potential impact. J. Hydrol. **295**: 64–86. doi:10.1016/j.jhydrol.2004.02.018

Smith, J. E., and others. 2006. Indirect effects of algae on coral: Algae-mediated, microbe-induced coral mortality. Ecol. Lett. **9**: 835–845. doi:10.1111/j.1461-0248.2006.00937.x

Smith, S. V., W. J. Kimmerer, E. A. Laws, R. E. Brock, and T. W. Walsh. 1981. Kaneohe Bay sewage diversion experiment: Perspectives on ecosystem responses to nutritional perturbation. Pac. Sci. **35**: 279–395.

Smith, S. V., and P. Kroopnick. 1981. Carbon-13 isotopic fractionation as a measure of aquatic metabolism. Nature **294**: 252–253. doi:10.1038/294252a0

Stieglitz, T. 2005. Submarine groundwater discharge into the near-shore zone of the Great Barrier Reef, Australia. Mar. Poll. Bull. **51**: 51–59. doi:10.1016/j.marpolbul.2004.10.055

Street, J. H., K. L. Knee, E. E. Grossman, and A. Paytan. 2008. Submarine groundwater discharge and nutrient addition to the coastal zone and coral reefs of leeward Hawai'i. Mar. Chem. **109**: 355–376. doi:10.1016/j.marchem.2007.08.009

Sunda, W. G., and W. J. Cai. 2012. Eutrophication induced CO_2-acidification of subsurface coastal waters: Interactive effects of temperature, salinity, and atmospheric pCO_2. Environ. Sci. Technol. **46**: 10651–10659. doi:10.1021/es300626f

Swarzenski, P. W., H. Dulaiova, M. L. Dailer, C. R. Glenn, C. G. Smith, and C. D. Storlazzi. 2013. A geochemical and geophysical assessment of coastal groundwater discharge at select sites in Maui and O'ahu, Hawai'i. *In* C. Wetzelhuetter [ed.], Groundwater in the coastal zones of Asia-Pacific. Springer.

University of Hawai'i at Mānoa, Department of Urban and Regional Planning (UH). 2002. Coral reefs located in marine waters around the main Hawaiian Islands. Hawai'i Statewide GIS Program. Available from http://www.state.hi.us/dbedt/gis/index.html

Venti, A., Kadko, D. A. J. Andersson, C. Langdon, C., and N. R. Bates. 2012. A multi-tracer model approach to estimate reef water residence times. Limnol. Oceanogr. Methods **10**: 1078–1095. doi:10.4319/lom.2012.10.1078

Wallace, R. B., H. Baumann, J. S. Grear, R. C. Aller, and C. J. Gobler. 2014. Coastal ocean acidification: The other eutrophication problem. Estuar. Coast. Shelf Sci. **148**: 1–13. doi:10.1016/j.ecss.2014.05.027

Wang, G., W. Jing, S. Wang, Y. Xu, Z. Wang, Z. Zhang, Q. Li, and M. Dai. 2014. Coastal acidification induced by tidal-driven submarine groundwater discharge in a coastal coral reef system. Environ. Sci. Technol. **48**: 13069–13075. doi:10.1021/es5026867

Wanninkhof, R. 1992. Relationship between wind speed and gas exchange over the ocean. J. Geophys. Res. Oceans **97**: 7373–7382. doi:10.1029/92JC00188

Weiss, R. 1974. Carbon dioxide in water and seawater: The solubility of a non-ideal gas. Mar. Chem. **2**: 203–215. doi: 10.1016/0304-4203(74)90015-2

Wisshak, M., C. H. Schönberg, A. Form, and A. Freiwald. 2012. Ocean acidification accelerates reef bioerosion. PloS One **7**: 45124. doi:10.1371/journal.pone.0045124

Wolanski, E., J. A. Martinez, and R. H. Richmond. 2009. Quantifying the impact of watershed urbanization on a coral reef: Maunalua Bay, Hawai'i. Estuar. Coast. Shelf Sci. **84**: 259–268. doi:10.1016/j.ecss.2009.06.029

Zeebe, R. E., and D. A. Wolf-Gladrow. 2001. CO_2 in seawater: Equilibrium, kinetics, isotopes. Gulf Professional Publishing.

Zektser, I. S., and H. A. Loaiciga. 1993. Groundwater fluxes in the global hydrologic cycle: Past, present and future. J. Hydrol. **144**: 405–427. doi:10.1016/0022-1694(93)90182-9

Acknowledgments

The authors thank David Ho, M. Dileep Kumar, and three anonymous reviewers for their valuable input on this manuscript. This project has been funded by grants from NOAA, Project #R/SB-11, which is sponsored by the University of Hawai'i Sea Grant College Program, SOEST, under Institutional Grant No. NA14OAR4170071(UNIHI-SEAGRANT-JC-15-01) from the NOAA Office of Sea Grant, Department of Commerce with additional support provided by the National Science Foundation Graduate Research Fellowship Program (DGE-1329626), and the Harold T. Stearns Fellowship. The views expressed herein are those of the authors and do not necessarily reflect the views of NOAA or any of its sub-agencies. This is SOEST publication number 10211.

Conflict of Interest

None declared.

Submitted 30 October 2016
Revised 07 April 2017
Accepted 01 June 2017

Associate editor: M. Dileep Kumar